



# LUND UNIVERSITY

## Further theoretical results on the stability of superheavy nuclei

Nilsson, Sven Gösta; Tsang, Chin Fu

*Published in:*  
Nuclear Physics, Section A

1970

[Link to publication](#)

*Citation for published version (APA):*  
Nilsson, S. G., & Tsang, C. F. (1970). Further theoretical results on the stability of superheavy nuclei. *Nuclear Physics, Section A*, (140), 289-304.

*Total number of authors:*  
2

### General rights

Unless other specific re-use rights are stated the following general rights apply:  
Copyright and moral rights for the publications made accessible in the public portal are retained by the authors and/or other copyright owners and it is a condition of accessing publications that users recognise and abide by the legal requirements associated with these rights.

- Users may download and print one copy of any publication from the public portal for the purpose of private study or research.
- You may not further distribute the material or use it for any profit-making activity or commercial gain
- You may freely distribute the URL identifying the publication in the public portal

Read more about Creative commons licenses: <https://creativecommons.org/licenses/>

### Take down policy

If you believe that this document breaches copyright please contact us providing details, and we will remove access to the work immediately and investigate your claim.

LUND UNIVERSITY

PO Box 117  
221 00 Lund  
+46 46-222 00 00

## FURTHER THEORETICAL RESULTS ON THE STABILITY OF SUPERHEAVY NUCLEI

CHIN FU TSANG and SVEN GÖSTA NILSSON<sup>†</sup>

*Lawrence Radiation Laboratory<sup>††</sup>, University of California, Berkeley, California 94720*

Received 3 October 1969

**Abstract:** Theoretical results are exhibited for the stability of superheavy nuclei with  $106 \leq Z \leq 128$  and  $176 \leq N \leq 204$  with respect to various decay mechanisms. A discussion is given of the production of superheavy nuclei by heavy-ion reactions. In particular, the experimental possibilities associated with the  $^{86}\text{Kr}$  beam are considered on the basis of the present calculations.

### 1. Introduction

Great interest in the study of superheavy nuclei was initiated by the work of Myers and Swiatecki<sup>1)</sup>, who showed that an island of stability against spontaneous fission may be expected around a region of doubly-closed nucleon shells. Several single-particle calculations<sup>2)</sup> suggested  $Z = 114$  and  $N = 184$  as the closest magic numbers beyond the region of known nuclei. The predicted island of stability around  $^{298}114_{184}$  is estimated to be centered near the extrapolated beta-stability line and may turn out to be accessible, if not by presently available accelerators and ions, by future experimental techniques.

A recent calculation<sup>3,4)</sup> exhibits the stability of nuclei in this region against spontaneous fission as well as against alpha and beta decays. It leads to the somewhat surprising result that some of these superheavy nuclei might have total half-lives comparable with the age of the solar system.

The shell-structure calculations also indicate a large energy gap in the neutron single-particle energy diagram at  $N = 196$  (for a discussion of the relevance of this subshell number see below). Thus the island of stability is predicted also to include the region associated with the neutron number  $N = 196$ , which region is not considered in ref. 4). In the present work we have thus enlarged our region of interest to that of nuclei with  $106 \leq Z \leq 128$  and  $176 \leq N \leq 204$ . Half-lives of spontaneous fission and alpha decay as well as the proton and neutron binding energies are calculated. Stability against beta decay is also investigated.

Ion beams such as  $^{64}\text{Ni}$ ,  $^{86}\text{Kr}$  and  $^{132}\text{Xe}$  may become available in accelerators of the near future. With appropriate targets these projectiles would produce compound nuclei in the region studied. A discussion is given of the possible experiments involving the  $^{86}\text{Kr}$  beam making use of the present theoretical results.

<sup>†</sup> On leave of absence from the Lund Institute of Technology, Lund, Sweden.

<sup>††</sup> Work performed under the auspices of the U. S. Atomic Energy Commission.

## 2. Method of calculation

The details of the calculation are described in ref. <sup>4</sup>). A generalised harmonic oscillator potential is employed with distortion coordinates  $\varepsilon$  and  $\varepsilon_4$  representing essentially  $P_2$  and  $P_4$  distortions in shape. In addition to the spin-orbit force, a shape correction term proportional to  $I^2 - \langle I^2 \rangle_N$  is also included, where the last term represents the average over a given oscillator shell. The strengths of the terms added to the oscillator potential represent two adjustable parameters for protons and two for neutrons, which are fitted to reproduce optimally the observed level order in the actinide ( $A \approx 242$ ) and the rare earth ( $A \approx 165$ ) regions. A linear  $A$ -dependence is assumed for these parameters for extrapolations to the superheavy region ( $A \approx 300-320$ ). Pairing energy contributions are calculated on the basis of the single-particle levels obtained. The pairing matrix element  $G$  is assumed to be isospin dependent and proportional to the surface area of the nucleus. The usually employed conservation of the volume of equipotential surfaces is complemented by the Strutinsky method of liquid-drop normalisation <sup>5</sup>). This method ensures that on the average the behavior of deformation energy is that given by a charged liquid drop. By employing correction terms in the normalisation function up to the sixth order, the final results are stable with respect to the range parameter employed in the normalisation <sup>4,6</sup>). The liquid-drop parameters are taken, without readjustment, from those of the semi-empirical mass formula of Myers and Swiatecki <sup>7</sup>).

## 3. Results of calculations

Basic to all of the calculations presented is the possibility to produce a reliable set of single-particle levels. In figs. 1 and 2 one may compare the level schemes predicted by the modified oscillator model with those obtained on the basis of a Woods-Saxon potential, as given in Rost <sup>8</sup>) (compare also, e.g., with those given by Bolsterli, Fiset and Nix <sup>9</sup>) and Chepurnov <sup>10</sup>). The proton level scheme there obtained is in good agreement with ours (see fig. 1). On the other hand the region of subshells around neutron number  $N = 184$  comes out somewhat different (fig. 2). Thus the  $h_{11/2}$  orbital is located relatively lower in our case, and, above this orbital,  $N = 196$  appears as a second subshell gap. Thus while the  $N = 184$  is associated with a larger energy gap in the references quoted, in our case the shell gap is split between the gaps of  $N = 184$  and  $N = 196$ . It turns out that the summed energy split across  $N = 184$  and  $N = 196$  is somewhat larger in our case. As can be seen from table 2 of the investigation by Muzychka <sup>11</sup>), different shell model prescriptions result in a remarkably close agreement in the height of the fission barrier peaks of the nuclei in the vicinity of  $Z = 114$  and  $N = 184$ . For  $N = 196$  the effect of the difference in level schemes predicted by the alternative potentials remains to be investigated quantitatively. It appears possible that the difference in barrier heights obtained might be more marked there than in the region investigated by Muzychka.

We have in the present investigation extended our calculations into this more

controversial region of extrapolation in spite of the discrepancy in level spacing predicted by the different potentials.

Potential-energy surfaces calculated in our model as a function of  $\varepsilon$  and  $\varepsilon_4$  deformations may be studied for each nucleus. In figs. 3a-h we exhibit the potential energy of isotopes of  $Z = 116, 120, 124$ , and  $128$  as a function of  $\varepsilon$  with minimization of energy with respect to  $\varepsilon_4$  for each value of  $\varepsilon$ . This type of plot represents a cut through

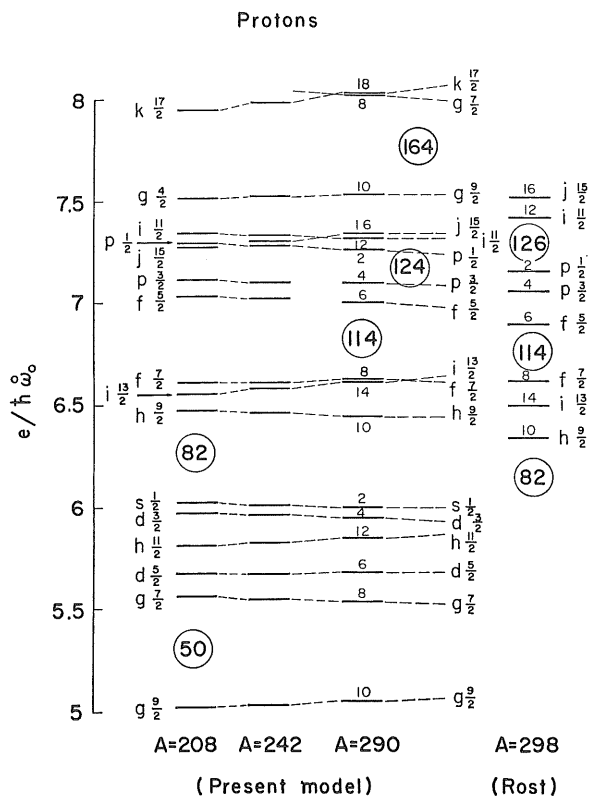


Fig. 1. Single-proton level diagram for spherical potential. Parameters are fitted <sup>4)</sup> to reproduce observed *deformed* single-particle level order at  $A \approx 165$  and  $242$  and are extrapolated linearly to the other regions. E. Rost's predicted level order <sup>8)</sup> for  $A = 298$  is exhibited for comparison.

the two-dimensional energy surface along the potential-energy minimum path with the energies projected onto the  $\varepsilon$ -axis. These figures should be compared with similar plots for isotopes of  $Z = 106$  up to  $Z = 116$  presented in ref. <sup>4)</sup>.

#### 4. Stabilities of nuclei with $106 \leq Z \leq 128$ and $176 \leq N \leq 204$

The energy of the lowest minimum in the potential-energy surface gives the ground state mass. Based on the masses obtained, alpha-decay half-lives, and neutron and proton binding energies are estimated. Beta stabilities are also determined. The

spontaneous-fission half-lives may also be found from the potential-energy surfaces provided one knows  $B$ , the inertial parameter associated with the barrier penetration. This parameter weighted by  $A^{-\frac{1}{2}}$  has been evaluated in three alternative ways. The first evaluation corresponds to the microscopic calculation due to Sobiczewski *et al.* <sup>12)</sup>, who found that the inertial parameters for the superheavy nuclei to cluster

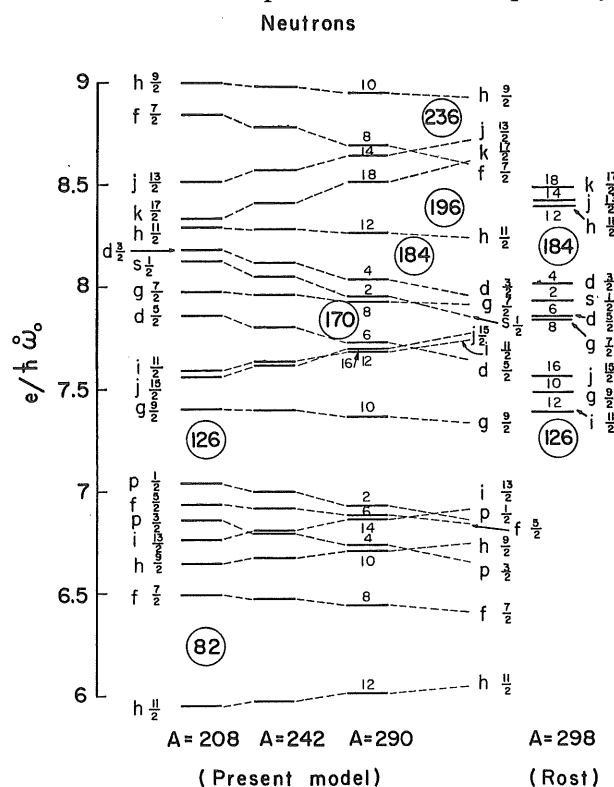


Fig. 2. Analogous to fig. 1, valid for neutrons.

within 30 % of a mean value in the actinide region. A second and semi-empirical estimate of  $BA^{-\frac{1}{2}}$  is obtained from the calculated barriers and the experimental half-lives. These inertial parameters are also found to cluster within 30 % of a mean value. A third estimate is due to Moretto and Swiatecki <sup>13)</sup>. They used liquid-drop barriers modified by the Myers-Swiatecki shell-correction term <sup>7)</sup> and with the ground state masses and fission barriers adjusted to experimental values. Moretto and Swiatecki determined the mean value of  $BA^{-\frac{1}{2}}$  for the actinides with only a 10 % spread. It is found that all of these three estimates lie within 30 % of each other, with the Moretto-Swiatecki estimate being the lowest. In our calculation of spontaneous-fission half-lives we have employed the latter estimate as giving the most conservative result. Based on the other estimates, some of the spontaneous-fission half-lives would be larger by one or two orders of magnitude.

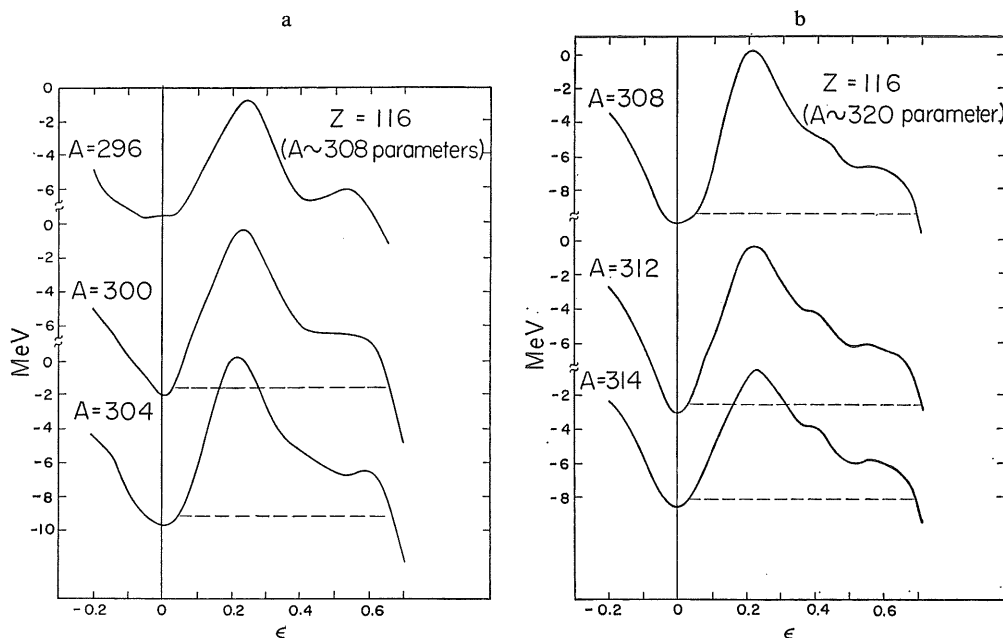


Fig. 3a. Total energy minimized with respect to  $\epsilon_4$  for each  $\epsilon$  as function of  $\epsilon$  for isotopes of  $Z = 116$  with  $N$  around 184.

Fig. 3b. Same as fig. 3a for isotopes of  $Z = 116$  with  $N$  around 196.

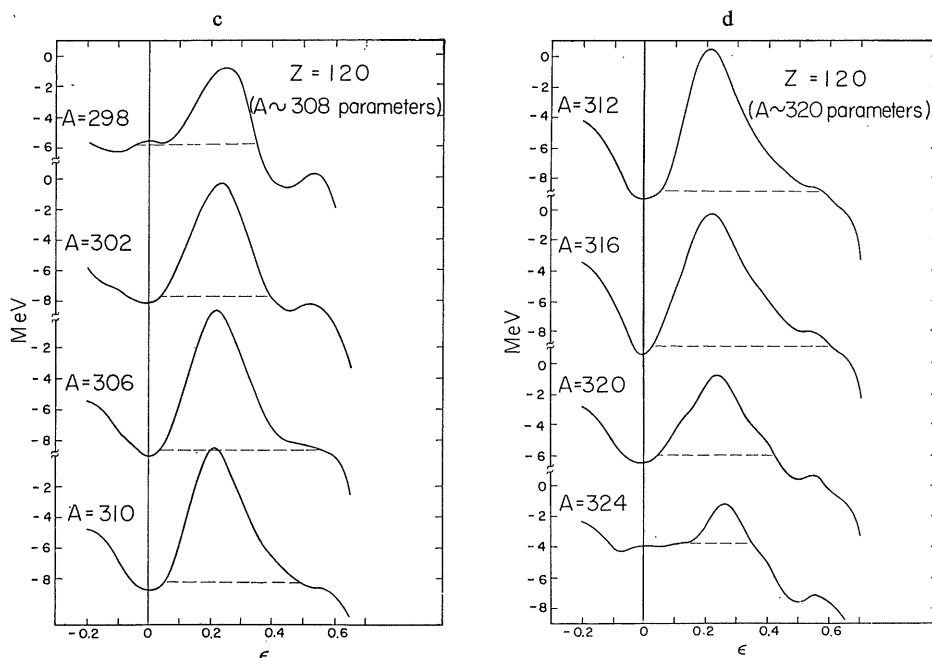


Fig. 3c. Same as fig. 3a for isotopes of  $Z = 120$  with  $N$  around 184.

Fig. 3d. Same as fig. 3a for isotopes of  $Z = 120$  with  $N$  around 196.

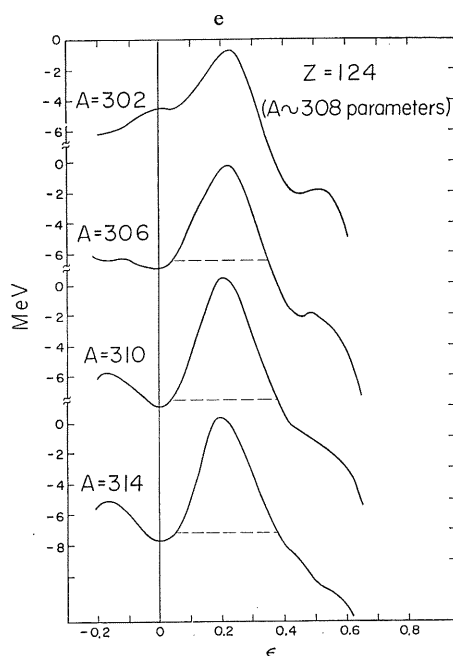
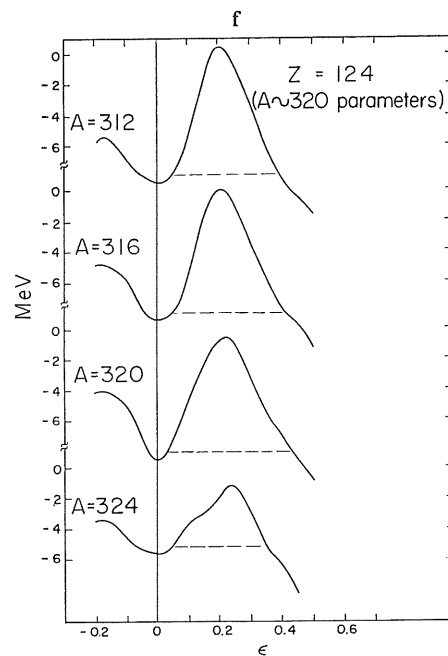
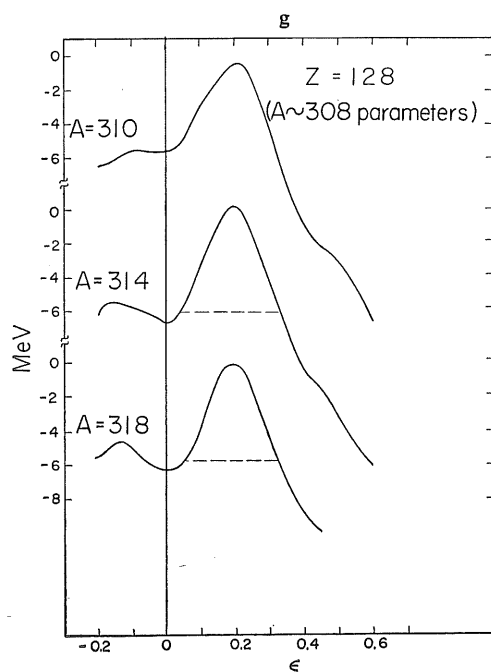
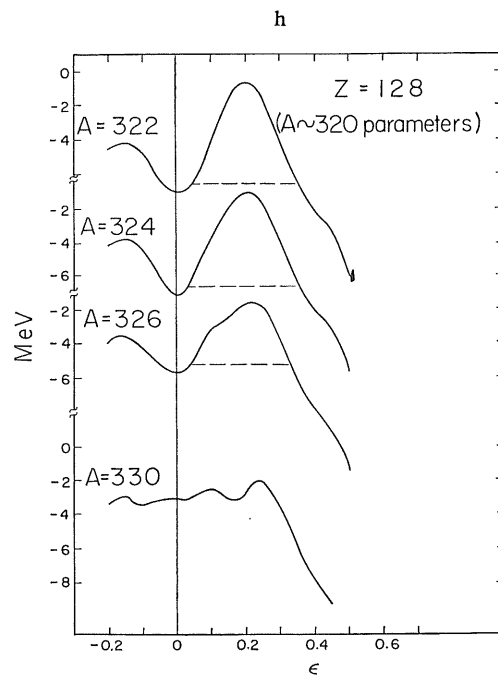
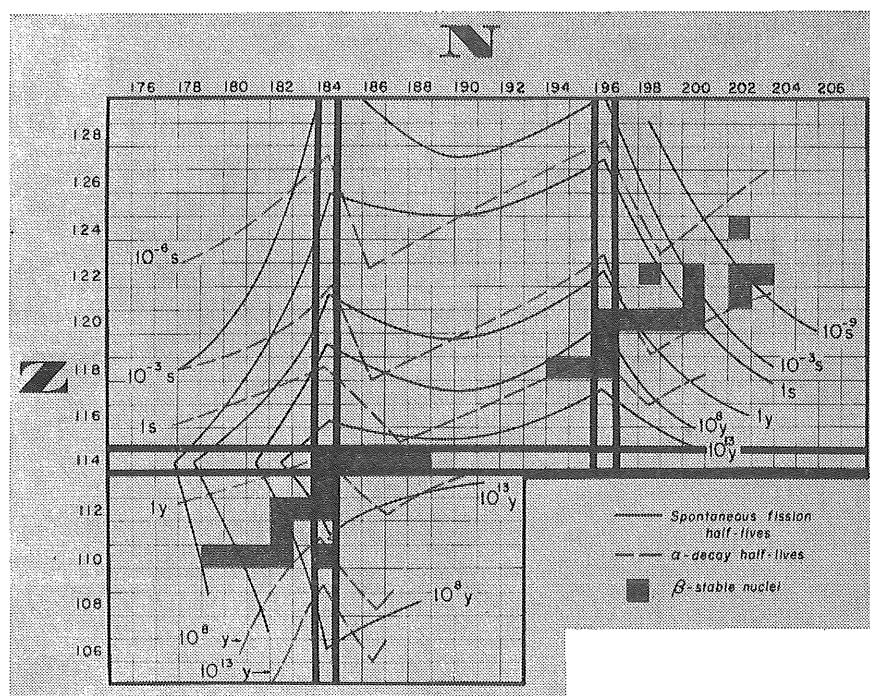
Fig. 3e. Same as fig. 3a for isotopes of  $Z = 124$  with  $N$  around 184.Fig. 3f. Same as fig. 3a for isotopes of  $Z = 124$  with  $N$  around 196.Fig. 3g. Same as fig. 3a for isotopes of  $Z = 128$  with  $N$  around 184.Fig. 3h. Same as fig. 3a for isotopes of  $Z = 128$  with  $N$  around 196.

Figure 1 shows a plot of the function  $f$  versus  $\epsilon$  for  $Z = 124$  (A ~ 320 parameters). The plot displays four curves, each corresponding to a different value of  $h$  (184, 196, 208, and 220). The curves are labeled 'h' at the bottom. The y-axis is labeled 'f' and the x-axis is labeled ' $\epsilon$ '. The curves show a sharp drop in  $f$  as  $\epsilon$  increases, with the drop occurring at higher  $\epsilon$  values for larger  $h$ .



The uncertainties associated with the calculated half-lives are discussed in detail

<sup>†</sup> The interesting recent calculations by Muzychka (Joint Institute of Nuclear Research, Dubna, Preprint R7-4435, 1969) employing three alternative nuclear potentials namely the Woods-Saxon potentials of refs. <sup>8)</sup> and <sup>10)</sup> in addition to the potential employed by us, exhibit a discrepancy in the prediction of alpha half-lives which in the most unfavorable cases may be as large a factor as  $10^8$ . On the whole, however, the discrepancy falls within the uncertainties expected according to ref. <sup>4)</sup>. One may note that in the  $^{294}110$  and  $^{298}114$  cases the discrepancy is of the order of  $10^4$ – $10^5$ . Finally one may note that the results based on our potential tend to fall between the predictions of the two alternative Woods-Saxon potentials employed.



TABLE

Table of masses, spontaneous-fission and alpha half-lives for  $116 \leq Z \leq 128$  and  $176 \leq N \leq 190$ . The upper line in each square gives the mass in MeV, the lower line the spontaneous-fission half-life and in parenthesis the barrier height in MeV. The third line in each square gives the alpha half-life in years, the fourth line the alpha energy in MeV and then the proton energy in MeV.

Z							
128							
127							
126							260.54 10 <sup>-4</sup> s (5.5) 10 <sup>-7</sup> s (14.1) , -0.39
125							252.86
124					243.41 (10 <sup>-4</sup> s) (5.2) 10 <sup>-6</sup> s (13.78) , +0.22	244.07	243.95 10 <sup>-3</sup> s (6.2) 10 <sup>-5</sup> s (13.1) 8.19, +0.3
123					236.34	236.92	236.98
122			227.20 (10 <sup>-3</sup> s) (5.0) 10 <sup>-5</sup> s (13.08) , +0.53	228.14	228.20 10 <sup>-5</sup> s (5.5) 10 <sup>-5</sup> s (13.09) 8.01, +0.71	228.96	228.94 10 <sup>-2</sup> s (7.0) 10 <sup>-4</sup> s (12.1) 8.09, +1.0
121			220.44	221.40	221.62	222.54	222.67
120	211.69 (10 <sup>-5</sup> s) (3.9)	212.68	212.68 (10 <sup>-5</sup> s) (5.0) 8.07, +1.17	213.77	214.04 10 <sup>-3</sup> s (6.3) 10 <sup>-4</sup> s (12.04) 7.80, +1.45	215.13	215.43 1s (7.3) 10 <sup>-3</sup> s (11.1) 7.77, +1.7
119		206.42	206.56	207.77	208.20	209.44	209.90
118			199.57 (10 <sup>-5</sup> s) (5.1) , +1.93	200.96	201.47 10 <sup>-2</sup> s (6.5) 10 <sup>-2</sup> s (10.91) 7.56, +2.18	202.89	203.50 10 <sup>5</sup> s (7.6) 0.1s (10.5) 7.46, +2.4
117			194.21	195.68	196.36	197.92	198.70
116			188.13 10 <sup>-3</sup> s (5.0)	189.76	190.53 10 <sup>6</sup> s (6.5) 7.30,	192.26	193.18 10 <sup>6</sup> y (7.9) 7.15,
Z/N	176	177	178	179	180	181	182

TABLE 1

8 and  $176 \leq N \leq 190$ . The upper  
The third line in each square gives  
energy and then the proton energy.

number in each square gives the mass excess in  $^{12}\text{C}$  scale (see ref. <sup>1</sup>) in MeV. In the line below is listed the  
the alpha half-life and the alpha  $Q$ -value (in parenthesis). The bottom line gives first the neutron binding en-  
Beta-stable nuclei are in italics.

				277.71 10 <sup>-2</sup> s (6.4) 10 <sup>-7</sup> s (14.74) , -0.74	278.42	278.59 10 <sup>-3</sup> s (6.2) 10 <sup>-9</sup> s (15.84) 7.90, -0.42	279.67	279.90 10 <sup>-4</sup> s (6.1) 10 <sup>-8</sup> s (15.62) 7.84, -0.09	281.23	281.61 10 <sup>-5</sup> s (5.7) 10 <sup>-8</sup> s (15.36) 7.69, 0.23	
				269.68	270.56	270.88	272.13	272.52	274.02	274.55	
	260.54 10 <sup>-4</sup> s (5.5) 10 <sup>-7</sup> s (14.70) , -0.39	260.69	260.32 0.1s (7.2) 10 <sup>-6</sup> s (13.94) 8.44, -0.08	261.35	261.85 10 <sup>-2</sup> s (7.2) 10 <sup>-8</sup> s (15.05) 7.57, 0.24	263.26	263.82 10 <sup>-3</sup> s (7.0) 10 <sup>-7</sup> s (14.83) 7.51, 0.56	265.47	266.18 10 <sup>-2</sup> s (6.6) 10 <sup>-7</sup> s (14.57) 7.36, 0.87		
	252.86	253.17	252.95	254.15	254.80	256.38	257.09	258.92	259.76		
(5.2) 3.78)	244.07	243.95 10 <sup>-3</sup> s (6.2) 10 <sup>-5</sup> s (13.32) 8.19, +0.32	244.43	244.37 10 <sup>2</sup> s (7.9) 10 <sup>-5</sup> s (13.00) 8.13, 0.64	245.73	246.56 10s (8.0) 10 <sup>-7</sup> s (14.12) 7.24, 0.98	248.30	249.18 1s (7.9) 10 <sup>-6</sup> s (13.88) 7.19, 1.29	251.16	252.18 0.1s (7.5) 10 <sup>-6</sup> s (13.61) 7.05, 161	
	236.92	236.98	237.61	237.72	239.26	240.25	242.14	243.18	245.33	246.50	
(5) 3.09) 7.71	228.96	228.94 10 <sup>-2</sup> s (7.0) 10 <sup>-4</sup> s (12.47) 8.09, +1.02	229.74	230.01 10 <sup>5</sup> s (8.6) 10 <sup>-3</sup> s (12.15) 7.80, 1.33	231.70	232.87 10 <sup>4</sup> s (8.6) 10 <sup>-6</sup> s (13.29) 6.90, 1.66	234.93	236.14 10 <sup>3</sup> s (8.5) 10 <sup>-5</sup> s (13.04) 6.86, 1.99	238.43	239.78 10s (8.2) 10 <sup>-5</sup> s (12.75) 6.72, 2.31	
	222.54	222.67	223.62	224.05	225.92	227.24	229.47	230.84	233.30	234.80	
(3) 2.04) 4.45	215.13	215.43 1s (7.3) 10 <sup>-3</sup> s (11.53) 7.77, +1.76	216.55	217.15 1y (9.0) 10 <sup>-2</sup> s (11.22) 7.47, +2.08	219.17	220.67 10y (9.1) 10 <sup>-4</sup> s (12.37) 6.57, 2.41	223.06	224.60 10 <sup>5</sup> s (8.9) 10 <sup>-4</sup> s (12.11) 6.53, 2.73	227.23	228.90 10 <sup>-1</sup> y (8.8) 10 <sup>-3</sup> s (11.83) 6.40, 3.05	
	209.44	209.90	211.19	211.94	214.14	215.79	218.35	220.04	222.84	224.66	
(5) 0.91) 1.18	202.89	203.50 10 <sup>5</sup> s (7.6) 0.1s (10.54) 7.46, +2.49	204.95	205.87 10 <sup>9</sup> y (9.2) 1s (10.26) 7.15, +2.82	208.23	210.06 10 <sup>8</sup> y (9.2) 10 <sup>-3</sup> s (11.43) 6.24, 3.15	212.78	214.64 10 <sup>7</sup> y (9.2) 10 <sup>-2</sup> s (11.15) 6.21, 3.47	217.59	219.59 10 <sup>5</sup> y (9.0) 10 <sup>-2</sup> s (10.87) 6.07	
	197.92	198.70	200.32	201.40	203.93	205.92	208.80	210.82			
	192.26	193.18 10 <sup>6</sup> y (7.9) 7.15,	194.95	196.20 10 <sup>12</sup> y (9.3) 6.82	198.89	201.06 10 <sup>12</sup> y (9.3) 5.90	204.11	206.29 10 <sup>11</sup> y (9.3) 5.89			
	181	182	183	184	185	186	187	188	189	190	N

TABLE 2  
Same as table 1, but for the region

Z							
128					285.13 0.1s (6.0) 10 <sup>-7</sup> s (14.65) ,0.85	286.73	287.81 10 <sup>-2</sup> s (5.5) 10 <sup>-6</sup> s (14.40) 6.99, 1.16
127					278.69	280.44	281.68
126	265.47 1s (7.5) 10 <sup>-7</sup> s (14.44) ,0.88	267.22	268.05 1s (7.2) 10 <sup>-6</sup> s (14.12) 7.24, 1.20	269.92	270.98 1s (6.8) 10 <sup>-6</sup> s (13.83) 7.01, 1.51	272.89	274.28 10s (6.5) 10 <sup>-5</sup> s (13.56) 6.68, 1.82
125	259.06	260.96	261.96	263.98	265.20	267.27	268.81
124	251.50 10s (8.3) 7.09, 1.61	253.57	254.72 10 <sup>2</sup> s (8.0) 10 <sup>-5</sup> s (13.15) 6.92, 1.93	256.91	258.29 10 <sup>4</sup> s (7.8) 10 <sup>-5</sup> s (12.86) 6.69, 2.23	260.51	262.22 10 <sup>3</sup> s (7.4) 10 <sup>-4</sup> s (12.59) 6.36, 2.55
123	245.82	248.05	249.36	251.71	253.23	255.62	257.48
122	239.14 10 <sup>6</sup> s (9.0) ,2.33	241.53	243.00 10 <sup>6</sup> s (8.9) 10 <sup>-4</sup> s (12.26) 6.6, 2.64	245.51	247.20 10 <sup>5</sup> s (8.6) 10 <sup>-3</sup> s (11.95) 6.38, 2.96	249.75	251.76 1y (8.2) 10 <sup>-2</sup> s (11.68) 6.06, 3.28
121	234.18	236.72	238.35	241.02	242.87	245.56	247.75
120	228.31 10 <sup>2</sup> y (9.4) ,3.09	231.02	232.82 10 <sup>4</sup> y (9.2) 10 <sup>-2</sup> s (11.31) 6.27, 3.41	235.65	237.65 10 <sup>4</sup> y (9.2) 10 <sup>-2</sup> s (11.00) 6.07, 3.72	240.51	242.84 10 <sup>8</sup> y (8.7) 0.1s (10.71) 5.74, 4.04
119	224.11	226.97	228.94	231.92	234.08	237.10	239.59
118	219.08 10 <sup>9</sup> y (9.7)	222.11	224.22 10 <sup>10</sup> y (9.5) 5.96, 4.16	227.37	229.70 10 <sup>10</sup> y (9.3) 10s (10.01) 5.74, 4.46	232.87	235.52 10 <sup>12</sup> y (9.0) 10s (9.73) 5.42, 4.79
117		218.83	221.09	224.40	226.87	230.21	233.02
116			217.26 10 <sup>15</sup> y (9.6)	220.71	223.36 10 <sup>16</sup> y (9.5) 5.42,	226.84	229.81 10 <sup>19</sup> y (9.2) 5.10,
Z/N	190	191	192	193	194	195	196

TABLE 2  
ne as table 1, but for the region

286.73	287.81 10 <sup>-2</sup> s (5.5) 10 <sup>-6</sup> s (14.40) 6.99, 1.16
280.44	281.68
272.89	274.28 10s (6.5) 10 <sup>-5</sup> s (13.56) 6.68, 1.82
267.27	268.81
260.51	262.22 10 <sup>5</sup> s (7.4) 10 <sup>-4</sup> s (12.59) 6.36, 2.55
255.62	257.48
249.75	251.76 1y (8.2) 10 <sup>-2</sup> s (11.68) 6.06, 3.28
245.56	247.75
240.51	242.84 10 <sup>8</sup> y (8.7) 0.1s (10.71) 5.74, 4.04
237.10	239.59
232.87	235.52 10 <sup>12</sup> y (9.0) 10s (9.73) 5.42, 4.79
230.21	233.02
226.84	229.81 10 <sup>19</sup> y (9.2) 5.10,

116 ≤ Z ≤ 128 and 190 ≤ N ≤ 204

290.37	292.32 10 <sup>-5</sup> s (3.6) 10 <sup>-8</sup> s (15.61) 6.12, 1.47	295.29	297.21 10 <sup>-11</sup> s (2.0) 10 <sup>-8</sup> s (15.34) 6.15, 1.78	300.21	302.05 10 <sup>-17</sup> s 10 <sup>-7</sup> s (14.67) 6.23, 2.17		
284.41	286.50	289.64	291.70	294.97	296.93	300.08	
277.17	279.44 10 <sup>-4</sup> s (4.7) 10 <sup>-8</sup> s (14.79) 5.80, 2.12	282.73	284.95 10 <sup>-8</sup> s (3.0) 10 <sup>-7</sup> s (14.51) 5.85, 2.44	288.39	290.66 <10 <sup>-13</sup> s (1.6) 10 <sup>-6</sup> s (14.07) 5.8, 2.76	293.96	296.13  10 <sup>-5</sup> s (13.16)
271.86	274.27	277.73	280.10	283.79	286.13	289.72	292.03
265.43	268.01 10 <sup>-1</sup> s (5.7) 10 <sup>-6</sup> s (13.82) 5.49 2.86	271.62	274.16 10 <sup>-6</sup> s (3.9) 10 <sup>-6</sup> s (13.54) 5.53, 3.18	278.01	280.54 10 <sup>-11</sup> s (2.5) 10 <sup>-5</sup> s (13.14) 5.54, 3.48	284.35	286.85 10 <sup>-17</sup> s 10 <sup>-4</sup> s (12.43) 5.57, 3.89
260.85	263.58	267.35	270.05	274.05	276.73	280.79	283.45
255.29	258.19 10 <sup>3</sup> s (6.4) 10 <sup>-5</sup> s (12.92) 5.17, 3.58	262.11	264.97 10 <sup>-4</sup> s (4.7) 10 <sup>-5</sup> s (12.63) 5.21, 3.91	269.14	271.99 10 <sup>-9</sup> s (3.1) 10 <sup>-4</sup> s (12.22) 5.22, 4.20	276.18	279.05 10 <sup>-15</sup> s (2.1) 10 <sup>-2</sup> s (11.64) 5.20, 4.58
251.42	254.48	258.57	261.59	265.91	268.90	273.34	276.34
246.68	249.91 10 <sup>4</sup> s (7.0) 10 <sup>-4</sup> s (11.96) 4.84, 4.35	254.15	257.34 1s (5.2) 10 <sup>-3</sup> s (11.68) 4.88, 4.66	261.81	264.98 10 <sup>-7</sup> s (3.6) 10 <sup>-2</sup> s (11.26) 4.90, 4.98	269.57	272.76 10 <sup>-11</sup> s (2.6) 0.1s (10.76) 4.88
243.59	246.97	251.38	254.71	259.36	262.67		
239.69	243.23 10 <sup>6</sup> y (7.5) 10 <sup>-2</sup> s (10.99) 4.53, 5.10	247.80	251.29 10s (5.6) 10 <sup>-1</sup> s (10.69) 4.58	256.08	259.57 10 <sup>-6</sup> s (4.0) 4.58		
237.35	241.04						
234.30	238.17 10 <sup>10</sup> y (7.5) 4.20,						
197	198	199	200	201	202	203	204 N

195 196

197 198 199 200 201 202 203 204 N

TABLE 3

Table of masses, spontaneous-fission and alpha half-lives near  $Z = 114$ ,  $N = 184$ . The upper number in each fission half-life and in parenthesis the barrier height in MeV. The bottom line in each square gives the

	178	179	180	181	182	$N$ 183
	187.87		190.36		193.14	
116	(1ms) (5.8)		1d (7.1)		$10^5$ y (8.3)	
	1s (10.14)		$\frac{1}{2}$ min (9.92)		10s (9.71)	
	183.02		185.75		188.85	
115			10 min (8.89)		10h (8.58)	
	178.01	180.09	181.00	183.17	184.41	186.56
114	1 min (5.4)		$10^2$ y (7.0)		$10^3$ y (8.3)	
			10d (7.97)	1y (7.71)	1y (7.55)	$10^2$ y (7.20)
	174.43		177.84		181.57	
113			10y (7.33)		$10^3$ y (6.80)	
	170.60	173.03	174.43	176.93	178.51	180.99
112	1s (4.1)		10d (5.7)		$10^6$ y (6.9)	
			1y (7.46)	$10^2$ y (7.17)	$10^3$ y (6.83)	$10^4$ y (6.52)
	168.08		172.34		176.83	179.47
111			10y (7.05)		$10^5$ y (6.38)	
$Z$						
	164.54	167.33	169.25	172.04	174.14	176.87
110	(1ms) (3.2)		10 min (4.3)		$10^4$ y (5.5)	
	10y (7.20)		$10^2$ y (6.85)	$10^4$ y (6.40)	$10^6$ y (6.14)	$10^9$ y (5.63)
	162.86		168.02	171.10	173.29	176.18
109						
	159.97	163.21	165.57	168.81	171.20	174.34
108			10s (3.2)		$10^2$ y (4.3)	
	$10^3$ y (6.38)		$10^4$ y (6.23)		$10^8$ y (5.57)	
107					171.20	174.49
					169.79	173.25
106					10d (3.9)	
					$10^{11}$ y (4.97)	

in ref. <sup>4</sup>). The predicted energy barrier may be overestimated because of the restricted parametrization, especially for large deformations. The estimation of  $B$  has an uncertainty of about 30 %. The calculated ground state masses for the known heavy nuclei are found <sup>4</sup>) to be good only to one or two MeV. All these errors enter into the half-life estimation exponentially, so that it is probable that our half-life values

TABLE 3

84. The upper number in each line in each square gives the

square gives the mass excess in  $^{12}\text{C}$  scale (see ref. <sup>1</sup>) in MeV. In the line below is listed the spontaneous-alpha half-life and the alpha  $Q$ -value (in parenthesis). Beta-stable nuclei are in italics. Taken from ref. <sup>4</sup>).

$N$		184	185	186	187	188	189
182	183						
193.14		196.42		201.30		206.55	
$10^5\text{y}$ (8.3)		$10^{11}\text{y}$ (9.4)		$10^{11}\text{y}$ (9.4)			
10s (9.71)		$\frac{1}{2}\text{min}$ (9.58)		0.1s (10.53)		1s (10.24)	
188.85		192.45		197.66		203.25	
10h (8.58)		1d (8.45)		10s (9.39)		10 min (9.11)	
184.41	186.56	<i>188.34</i>	<i>191.29</i>	<i>193.88</i>	<i>197.32</i>	<i>199.84</i>	203.52
$10^9\text{y}$ (8.3)		$10^{16}\text{y}$ (9.6)		$10^{15}\text{y}$ (9.4)		$10^{14}\text{y}$ (9.4)	
1y (7.55)	$10^2\text{y}$ (7.20)	10y (7.40)	100d (7.87)	1d (8.34)	5h (8.49)	10d (8.09)	10d (8.00)
181.57		<i>185.84</i>		191.71		198.00	
$10^3\text{y}$ (6.80)		$10^5\text{y}$ (6.58)		1y (7.53)		10y (7.29)	
<i>178.51</i>	<i>180.99</i>	<i>183.11</i>	186.40	189.32	193.09	195.94	199.95
$10^6\text{y}$ (6.9)		$10^{13}\text{y}$ (8.1)		$10^{13}\text{y}$ (8.1)		$10^{12}\text{y}$ (8.1)	
$10^3\text{y}$ (6.83)	$10^4\text{y}$ (6.52)	$10^4\text{y}$ (6.54)	$10^2\text{y}$ (7.10)	1y (7.50)	100d (7.65)	10y (7.24)	10y (7.16)
<i>176.83</i>	<i>179.47</i>	181.75		188.28		195.23	
$10^5\text{y}$ (6.38)		$10^7\text{y}$ (6.03)		$10^2\text{y}$ (6.98)		$10^3\text{y}$ (6.72)	
<i>174.14</i>	176.87	<i>179.39</i>	183.01	186.27	190.36	193.54	197.88
$10^4\text{y}$ (5.5)		$10^{10}\text{y}$ (6.8)		$10^{10}\text{y}$ (5.7)		$10^9\text{y}$ (6.8)	
$10^6\text{y}$ (6.14)	$10^9\text{y}$ (5.63)	$10^8\text{y}$ (5.76)	$10^5\text{y}$ (6.24)	$10^2\text{y}$ (6.73)	$10^2\text{y}$ (6.86)	$10^4\text{y}$ (6.45)	$10^4\text{y}$ (6.35)
173.29	176.18	178.87	182.66	186.08		193.68	
		$10^{11}\text{y}$ (5.24)		$10^5\text{y}$ (6.21)			
171.20	174.34	177.11	181.07	184.66	189.10	192.60	
$10^2\text{y}$ (4.3)		$10^8\text{y}$ (5.8)		$10^8\text{y}$ (5.9)		$10^7\text{y}$ (5.8)	
$10^8\text{y}$ (5.57)		$10^{13}\text{y}$ (4.89)	$10^9\text{y}$ (5.39)	$10^6\text{y}$ (5.86)			
171.20	174.49	177.44					
169.79	173.25	176.37					
10d (3.9)		$10^7\text{y}$ (5.3)					
$10^{11}\text{y}$ (4.97)							

se of the restricted  
a of  $B$  has an un-  
the known heavy  
e errors enter into  
ur half-life values

may be off by about four or five powers of ten. To this is then added the uncertainty due to the extrapolation of the nuclear potential to new mass regions. Nevertheless we expect the general pattern of the half-life contours to remain the same so long as  $Z = 114$ ,  $N = 184$  and  $N = 196$  are associated with relatively large level spacings. Then the map should be useful as a guide in the search for superheavy nuclei.

### 5. Production of superheavy nuclei by heavy-ion reactions

The production of superheavy nuclei by various methods is discussed in refs. <sup>4,14</sup>). At the moment it appears that the most promising method is associated with heavy-ion reactions.

With the presently available heavy-ion beams, the heaviest being that of  $^{40}\text{Ar}$ , one finds that the compound nucleus produced is very neutron-deficient and therefore falls short of the island of stability. When heavier and hence more neutron-rich ions

TABLE 4  
Production of superheavy nuclei by  $^{86}\text{Kr}_{50}$  projectile

Target	Compound nucleus			After emitting 4n		Longest-lived nuclei reached after competition between s.f. and successive $\alpha$ -decay			After $\beta$ -decay		
	A	Z	N	Z	N	Z	N	major decay	Z	N	major decay
Pb	208	82	126	118	176	118	172	(s.f)			
Po	210	84	126	120	176	120	172	(s.f)			
Rn											
Ra	226	88	138	124	188	124	184	118 178 $\alpha(10^{-3}\text{s})$	112	184	$\alpha(10^4\text{y})$
Th	232	90	142	126	192	126	188	116 178 $\alpha(10^{-1}\text{s})$	112	182	$\alpha(10^2\text{y})$
U	238	92	146	128	196	128	192	114 178 $\alpha(10^3\text{s})$	110	182	$\alpha(10^2\text{y})$
Pu	244	94	150	130	200	130	196	114 180 $\alpha(10^4\text{s})$	112	182	$\alpha(10^2\text{y})$
Cm	248	96	152	132	202	132	198	114 180 $\alpha(10^4\text{s})$	112	182	$\alpha(10^2\text{y})$

Production of superheavy nuclei by  $^{86}\text{Kr}_{50}$  beam. The first column identifies the target nucleus. The second column indicates the compound nucleus that is formed by the fusion of the target and the projectile. Assuming that all the excitation energy might be carried away by the emission of four neutrons the nucleus shown in the third column is obtained. Under the additional assumption that beta decays are negligibly slow compared with spontaneous fission and alpha decay the longest lived superheavy nucleus that can be reached is shown in the fourth column with its major mode of decay. Under the further assumption that the nucleus in column 4 undergoes beta decay the superheavy nucleus shown in the fifth column is obtained with its major mode of decay as indicated.

than  $^{40}\text{Ar}$  can be accelerated, the prospect is improved for the production of superheavy nuclei. A plausible way of approach is to overshoot the  $^{298}114$  doubly-closed shell nucleus and let various decay mechanisms lead up to a nucleus in its neighborhood. An extreme example is the reaction  $^{238}\text{U} + ^{238}\text{U}$ , as pointed out by Flerov [ref. <sup>15</sup>)], Swiatecki <sup>16</sup>) and others. One may then expect that either a transfer reaction takes place, where the target captures a part of the projectile, or a compound nucleus is formed, which then undergoes fission. One hopes in this way to find products that are close enough to the center of the island of stability to have half-lives long enough for detection.

A possibility that is not so remote is furnished by reactions induced by the  $^{86}\text{Kr}$  ion beam. In table 4 we show the compound nuclei that might be formed by bombarding various neutron-rich targets from Pb to Cm with  $^{86}\text{Kr}$ . The question whether

ions

ssed in refs. <sup>4,14</sup>).  
ciated with heavy-

ing that of <sup>40</sup>Ar,  
cient and therefore  
neutron-rich ions

After  $\beta$ -decay

ay

Z	N	major decay
---	---	----------------

112	184	$\alpha(10^4\text{y})$
112	182	$\alpha(10^2\text{y})$
110	182	$\alpha(10^2\text{y})$
112	182	$\alpha(10^2\text{y})$
112	182	$\alpha(10^2\text{y})$

the target nucleus. The  
of the target and the  
the emission of four  
onal assumption that  
decay the longest lived  
major mode of decay.  
decay the superheavy  
indicated.

roduction of super-  
114 doubly-closed  
nucleus in its neigh-  
bored out by Flerov  
either a transfer  
le, or a compound  
this way to find  
bility to have half-

duced by the <sup>86</sup>Kr  
rmed by bombard-  
question whether

such a compound nucleus would be formed in the first place will be touched on below. At the moment let us assume that by emitting four neutrons a cold compound nucleus is obtained in the ground state. From fig. 4, it is apparent that for <sup>208</sup>Pb and <sup>210</sup>Po targets, the compound nucleus undergoes spontaneous fission instantaneously and one may not expect to produce any superheavy nuclei. With targets heavier than <sup>226</sup>Ra, it turns out that the alpha half-life is less than the spontaneous-fission half-life at each step (fig. 4). If the compound nucleus decays by emitting alpha particles all the way, in each case we end up with a long-lived superheavy nucleus. Any beta decay on the way, if competitive, will always help in reaching even longer-lived nuclei.

It is here appropriate again to emphasize that fig. 4 and the conclusions based thereon depend strongly on the magnitude of the  $N = 196$  shell spacing which, as stated earlier, is a controversial result obtained on the basis of our specific potential model, which at this point disagrees with alternative potentials.

The above discussion of the production of superheavy nuclei is based on the assumption that the compound nucleus is formed with sufficient probability in the reaction. This assumption may be subject to question for the following reasons. (1) There exist empirical indications that the cross section of reactions, leading to the same compound nucleus, with a heavy projectile is reduced by several orders of magnitude compared with a reaction in which a lighter projectile is employed. (2) The large angular momentum introduced with the heavy projectile may cause the compound nucleus to fission directly rather than to decay into a stable minimum. This tendency is found in the liquid-drop model calculations, e.g., those of Cohen, *et al.* <sup>17</sup>). (3) Furthermore we know that any binding of a superheavy nucleus is due to so-called "shell contributions" connected with the doubly closed shells. The problem is somewhat open whether possibly these "shell contributions" are affected at the relatively large excitation of the compound nucleus in question.

Further studies of these problems are essential for any further attempts to make definite theoretical proposals for the production of superheavy nuclei.

We are much indebted to Dr. W. J. Swiatecki for stimulating and constructive discussions at various phases of this work. We are also grateful to Drs. G. T. Seaborg and S. G. Thompson for stimulating encouragement. The co-operation of Drs. A. Sobiczewski, Z. Szymanski, S. Wycech, C. Gustafson, I. L. Lamm, P. Möller, and B. Nilsson is deeply appreciated.

The friendly hospitality of the Nuclear Chemistry Division and its excellent publication services are gratefully acknowledged.

### References

- 1) W. D. Myers and W. J. Swiatecki, Nucl. Phys. **81** (1966) 1
- 2) H. Meldner and P. Röper, private communication to W. D. Myers and W. J. Swiatecki (see ref. <sup>1</sup>);  
H. Meldner, Ark. Fys. **36** (1967) 593, Lawrence Radiation Laboratory Report UCRL-17801 (October 1968);



- A. Sobiczewski, F. A. Gareev, and B. N. Kalinkin, Phys. Lett. **22** (1966) 500;  
V. M. Strutinsky and Yu. A. Muzychka, Proc. Int. Conf. of the physics of heavy ions, 13-19 October (1966), Dubna, Vol. 2, p. 51;  
C. Y. Wong, Phys. Lett. **21** (1966) 688;  
C. Gustafson, I. L. Lamm, B. Nilsson, and S. G. Nilsson, Ark. Fys. **36** (1967) 613; the shell closing at  $Z = 114$  is already apparent from fig. 5 of B. R. Mottelson and S. G. Nilsson, Mat. Fys. Skr. Dan. Vid. Selsk. **1** (1959) No. 8
- 3) S. G. Nilsson, J. R. Nix, A. Sobiczewski, Z. Szymanski, S. Wycech, C. Gustafson and P. Möller, Nucl. Phys. **A115** (1968) 545
  - 4) S. G. Nilsson, C. F. Tsang, A. Sobiczewski, Z. Szymanski, S. Wycech, C. Gustafson, I. L. Lamm, P. Möller and B. Nilsson, Nucl. Phys. **A131** (1969) 1;  
S. G. Nilsson, Lawrence Radiation Lab. Rep. UCRL-18355-Rev. (Berkeley, Sept. 1968);  
S. G. Nilsson, S. G. Thompson and C. F. Tsang, Phys. Lett. **28B** (1969) 548
  - 5) V. M. Strutinsky, Nucl. Phys. **A95** (1967) 420; Nucl. Phys. **A122** (1968) 1
  - 6) C. F. Tsang, Ph. D. Thesis, University of California Lawrence Radiation Lab. Rep. UCRL-18899
  - 7) W. D. Myers and W. J. Swiatecki, Lysekil Symposium, Sweden, 1966, (Almqvist and Wiksell, Stockholm, 1967), p. 393 and Ark. Fys. **36** (1967) 593
  - 8) E. Rost, Phys. Lett. **26B** (1967) 184
  - 9) M. Bolsterli, E. O. Fiset, and J. R. Nix, Los Alamos Scientific Lab. Rep. LA-DC-10249 (1969)
  - 10) V. A. Chepurinov, Yad. Fiz. **6** (1967) 955
  - 11) Yu. A. Muzychka, Phys. Lett. **28B** (1969) 539
  - 12) A. Sobiczewski, Z. Szymanski, S. Wycech, S. G. Nilsson, J. R. Nix, C. F. Tsang, C. Gustafson, I. L. Lamm, P. Möller and B. Nilsson, Nucl. Phys. **A131** (1969) 67
  - 13) L. G. Moretto and W. J. Swiatecki, private communication
  - 14) G. T. Seaborg, Ann. Rev. Nucl. Sci. **18** (1968) 53-152
  - 15) G. N. Flerov, JINR, Dubna, preprint E7-4207 (1968)
  - 16) W. J. Swiatecki, Research Progress Meeting Talk, Lawrence Radiation Lab., Berkeley, February 1968
  - 17) S. Cohen, F. Plasil and W. J. Swiatecki, Proc. Third Int. Conf. on reactions between complex nuclei, University of California Press, Berkeley (1963) 325

Fysik & astronomi  
Lunds universitet